THE ASTRONOMICAL JOURNAL VOLUME 112, NUMBER 5 NOVEMBER 1996

ANGULAR SIZE MEASUREMENTS OF 18 MIRA VARIABLE STARS AT 2.2 μm

G. T. VAN BELLE[1] AND H. M. DYCK

Department of Physics and Astronomy, University of Wyoming, Laramie, Wyoming 82071
Electronic mail: vanbelle@uwyo.edu, meldyck@uwyo.edu

J. A. BENSON

USNO, Flagstaff Station, POB 1149, Flagstaff, Arizona 86002-1149
Electronic mail: jbenson@nofs.navy.mil

M. G. LACASSE

FLWO, Smithsonian Institution, P.O. Box 97, Amado, Arizona 85645
Electronic mail: mlacasse@cfa.harvard.edu

Received 1996 May 17; revised 1996 August 5

ABSTRACT

We present angular size measurements of 18 oxygen-rich Mira variable stars. These data are part of a long term observational program using the Infrared Optical Telescope Array (IOTA) to characterize the observable behavior of these stars. Complementing the infrared angular size measurements, values for variable star phase, spectral type, bolometric flux, and distance were established for stars in the sample; flux and distance led to values for effective temperature ($T_{\rm EFF}$), and linear radius, respectively. We are able to define an effective temperature versus spectral type scale for Mira variables that we compare to the temperature scales for K and M giants and supergiants. $T_{\rm EFF}$'s and linear radii for these stars are shown to lie between approximately 2100 and 3200 K, and 200 and 600 $R_\odot$, respectively. Relationships among the Mira variable parameters are explored for significant trends. Notably, the phase dependence of $T_{\rm EFF}$ is shown to follow simple expectations, and examination of the radius–$T_{\rm EFF}$ relationship yields a plausible description of the V and K band light curves of these stars. A simple examination of the oscillation mode of the stars in the sample does not strongly suggest either fundamental or first-overtone oscillation as the primary mode of oscillation. This conclusion differs from that recently presented by Haniff *et al.* (1995), who argue that Mira variables are all first-overtone pulsators. We discuss some possible reasons for the different conclusions between the two studies.

1. INTRODUCTION

The recent development of interferometric methods at optical and infrared wavelengths has provided the astronomical community with more than an order of magnitude increase in spatial resolution over direct imaging techniques. Using the Infrared Optical Telescope Array (IOTA, see Carleton *et al.* 1994 and Dyck *et al.* 1995), we have recently begun a program of high-resolution, K-band observations of Mira variable stars. Mira variables figure prominently in our observing strategy, since these stars are large and bright at infrared wavelengths. Using crude estimates of surface temperatures and the observed total fluxes it is estimated that more than 70 such stars have blackbody angular diameters in excess of 5 milliarcseconds (mas), easily resolvable targets for the current generation of Michelson interferometers. However, only six JHK band diameters for five of these stars have been published in the literature (Ridgway *et al.* 1979; Di Giacomo *et al.* 1991; Ridgway *et al.* 1992); the data on the 18 stars presented in this paper more than triple the existing sample of measured angular diameters for Mira variables at near-infrared wavelengths. More importantly, this large sample allows for more detailed analyses of the behavior of these stars.

Recent models of Mira variables have attempted to resolve important questions regarding the pulsation mode, mass loss, and evolution of these stars. The pulsation mode remains a currently unresolved issue; depending upon initial assumptions, models supporting both fundamental mode oscillation (Willson & Hill 1979; Hill & Willson 1979; Wood 1990) and first-overtone oscillation (Wood 1974; Tuchman *et al.* 1979; Perl & Tuchman 1990) have been constructed. Attempts to reconcile the models with observations have produced results in support of both fundamental mode (Cannizzo *et al.* 1990) and first-overtone pulsation (Tuchman 1991; Barthès & Tuchman 1994; Haniff, Scholz & Tuthill 1995). In addition to addressing the question of oscillation mode, stellar evolution questions, such as the connection of Mira variable star mass loss rates to planetary nebula formation, have also been explored (Tuchman *et al.* 1979).

It is by means of *direct observation* of the angular sizes of Mira variables that we may be able to provide unique insight into these questions. For example, recent studies at optical wavelengths (Haniff *et al.* 1995, hereafter referred to as

[1]NASA Space Grant Fellow.

 0004-6256/96/112(5)/2147/12/$10.00

HS&T) have attempted to infer the mode of pulsation from the diameter data. Additional information in the form of bolometric flux estimates will yield further information, such as effective temperature, the scale for which is not particularly well established for this class of stars. Also, our angular size measurements and derived quantities have implications regarding the nature of mass loss and evolution among Mira variables. An investigation of mass loss evolution by Bowen & Willson (1991) used indirectly-inferred values for stellar radius and effective temperature, both of which are more directly obtained in this investigation.

Carbon-rich, oxygen-rich, and S-type Miras are all being observed at IOTA as a part of our ongoing high-resolution program; in this paper we present only the observations of the oxygen-rich variety. Operations at IOTA producing these results are discussed in Sec. 2, detailing source selection and observation. In Sec. 3 the procedures used in establishing the stellar parameters for the stars observed are discussed; the parameters include phase, spectral type, bolometric flux, angular size, effective temperature, and linear radius. These parameters are in turn examined for significant interrelationships in the discussion of Sec. 4. Under the assumption of the validity of the period–mass–radius relations developed by Ostlie & Cox (1986), the IOTA data collected on the Mira variables observed in this program do not strongly indicate a particular oscillation mode. This result differs substantially from the results of a comparable study by HS&T, who conclude that Mira variables are first-overtone pulsators; we discuss the implications of these differences in Sec. 4.

2. OBSERVATIONS

The data reported in this paper were obtained in the K band ($\lambda=2.2$ μm, $\Delta\lambda=0.4$ μm) at IOTA, using the 38 m baseline. Use of IOTA at 2.2 μm to observe Mira variables offers three advantages: First, effects of interstellar reddening are minimized, relative to the visible ($A_K=0.11\ A_V$; Mathis 1990); second, the effects of circumstellar emission are minimized shortward of 10 μm (Rowan-Robinson & Harris 1983), and; third, the K-band apparent uniform-disk diameter of Mira variables is expected to be close to the Rosseland mean photospheric diameter (see the discussion in Sec. *3.3*). The interferometer, detectors, and data reduction procedures have been described more fully by Carleton *et al.* (1994) and Dyck *et al.* (1995). As was previously reported in these papers, starlight collected by the two 0.45 m telescopes is combined on a beam splitter and detected by two single-element InSb detectors, resulting in two complementary interference signals. The optical path delay is mechanically driven through the white light fringe position to produce an interferogram with fringes at a frequency of 100 Hz. Subsequent data processing locates the fringes in the raw data and filters out the low- and high-frequency noise with a square filter 50 Hz in width. Recent software and hardware upgrades to the computers driving the interferometer and collecting the data have resulted in a improved data collection rate to 1500–2000 fringe packets per night. On the best nights we can observe 20 science sources and an equal number of calibrators.

Observations of target objects are alternated with observations of unresolved calibration sources to characterize slight changes in interferometer response, due to both seeing and instrumental variations. Raw visibilities are determined from the amplitude of the interferogram at the white light fringe position, normalized by the incoherent flux from the star. An estimate of the noise is obtained from a similar measurement made in the data string outside the region of coherence; the noise estimate is used in obtaining a weighted average of the visibility data, which is typically taken in sets of 50 interferograms. The raw visibilities of the target objects are then calibrated by dividing them by the measured visibilities of the calibration sources, using the calibration sources as samples of the interferometer's point response. Calibration sources were selected from V-band data available in *The Bright Star Catalog, 4th Revised Edition* (Hoffleit 1982) and K-band data in the *Catalog of Infrared Observations* (Gezari *et al.* 1993), based upon angular sizes calculated from estimates of bolometric flux and effective temperature; calibration source visibility was selected to be at least 90% and ideally greater than 95%, limiting the effect of errors in calibrator visibility to a level substantially below measurement error.

Mira variables observed for this paper were selected based upon a number of criteria. Stars needed to be bright enough in V and K to be detected by both the star trackers and the InSb detectors; the current limits of the IOTA interferometer dictate $V<8.0$ mag and $K<5$ mag (though for observations at all airmasses and seeing conditions, we require $K<2.5$ mag). The Mira variables needed to be at a declination accessible to the mechanical delay available for a given evening. This is because the difference in delay between the two apertures, which can range from -30 to $+20$ m, depends upon source declination and hour angle. Since only 4.6 m of this range is accessible at any time, observing is constrained to a specific declination bin about 10° wide on any given night. The stars also needed to be of sufficient estimated angular size to be resolved by IOTA. Mira phase was not a factor in target selection; hence, our targets represent Miras at a variety of phases, from visible light maximum to minimum.

Eighteen oxygen-rich Mira variables were observed at IOTA during three observing runs in June, July, and October of 1995. The visibility data for the two detector channels have been averaged and are listed in Table 1, along with the date of the observation, the interferometer projected baseline, the stellar phase, and the derived uniform disk angular size; the latter two points are discussed further in Sec. 3. Our experience with the IOTA interferometer (Dyck *et al.* 1996) has demonstrated that the night-to-night rms fluctuations in visibility data generally exceed the weighted statistical error from each set of interferograms; we have characterized these fluctuations and use the empirical formula

$$\epsilon_V = \pm \frac{0.0509}{\sqrt{\text{number of nights}}} \quad (1)$$

to assign the "external" error. The interested reader should see Dyck *et al.* (1996) for a more complete discussion. Finally, visibility data were fit to uniform disk models to obtain

TABLE 1. The observed data.

Star	P [d]	Date	B_p [m]	V^1	ϕ	θ_{UD} [mas]
R Aql	283.4	95 Jun 10	36.24	0.3255	0.90	10.76±0.61
		95 Jun 11	35.76	0.3437		
		95 Oct 06	33.85	0.1657	0.31	13.62±0.72
R Aqr	387.8	95 Jul 11	31.51	0.1404	0.34	14.95±0.93
		95 Jul 11	29.48	0.2125		
		95 Oct 07	33.19	0.1540	0.57	14.06±0.72
R Aur	457.4	95 Oct 03	35.16	0.3050	0.08	11.06±0.58
		95 Oct 04	34.91	0.3522		
		95 Oct 05	35.92	0.3146		
R Cas	430.8	95 Oct 04	35.27	0.1245	0.81	13.55±0.95
		95 Oct 05	36.30	0.1273		
T Cas	445.0	95 Oct 04	35.33	0.1835	0.30	12.81±0.66
S Her	308.5	95 Jul 07	36.50	0.7914	0.81	4.85±1.17
		95 Jul 08	36.96	0.8630		
U Her	406.4	95 Jun 10	36.84	0.2998	0.03	10.65±0.79
		95 Jun 13	36.94	0.3797		
X Oph	331.6	95 Jul 07	35.53	0.1289	0.37	12.97±0.60
		95 Jul 08	36.59	0.1535		
		95 Oct 07	34.11	0.2571	0.75	12.30±0.76
S Ori	413.4	95 Oct 06	33.86	0.3313	0.56	10.54±0.68
		95 Oct 07	32.96	0.5149		
U Ori	371.4	95 Oct 08	38.24	0.2480	0.97	11.08±0.57
R Peg	377.3	95 Jul 07	36.65	0.3909	0.90	10.18±0.40
		95 Jul 08	36.84	0.3109		
		95 Oct 06	34.49	0.4199	0.13	9.72±0.67
		95 Oct 07	34.50	0.5116		
S Peg	320.0	95 Jul 08	36.58	0.5766	0.28	7.90±0.72
		95 Oct 06	34.01	0.7294	0.56	6.32±0.95
		95 Oct 07	34.00	0.7712		
U Per	322.4	95 Oct 04	35.55	0.7763	0.55	5.84±0.78
		95 Oct 05	36.02	0.7358		
R Ser	355.4	95 Jul 07	36.50	0.4873	0.32	8.56±0.58
		95 Jul 08	36.89	0.5429		
X Aur	164.0	95 Oct 04	34.98	1.1506	0.62	Unresolved
Z Cet	185.2	95 Oct 06	32.87	0.9998	0.92	Unresolved
RY Lyr	326.6	95 Oct 08	38.26	1.0858	0.37	Unresolved
R Per	210.1	95 Oct 05	37.00	1.1585	0.03	Unresolved

1. Standard nightly error is $\epsilon_V = 0.0509$.

an initial angular size θ_{UD}. These uniform disk diameters and their estimated errors, derived from the uncertainty in the visibilities, are also listed in Table 1.

We note that typically a single point was utilized in calculating the uniform disk diameter θ_{UD}. For the stars in our sample, the visibility data were all at spatial frequencies, x, shortward of the first zero of the uniform disk model, $|2J_1(x)/x|$. HS&T noted that the uniform disk model was not a particularly good model for visible-light data for Mira variables; rather, the data were a better fit to a simple Gaussian. Although we do not currently have multiple spatial frequency data for any Mira variables, we expect that the departures from a uniform disk model will not be as great at 2.2 μm as it is at visible wavelengths. This expectation is based upon our unpublished 2.2 μm data for α Her, a supergiant star expected to have the same order of atmospheric extension as do the Mira variables. A comparison of our data with visible α Her data (Tuthill 1994) indicates that the departures from a uniform disk visibility curve are present in the visible but not the infrared. Thus we assume that to first order, a uniform disk model will also fit the Mira data; a slight correction to the derived angular sizes to account for this assumption will be discussed in Sec. *3.3*. In this case, a single spatial frequency point will uniquely and precisely determine the angular diameters for visibilities in the approximate range $0.25 \leq V \leq 0.75$. If there are significant differences between the brightness profiles for supergiants and for Mira variables then this assumption will be invalid; this point may only be addressed by detailed multiple spatial frequency observations of the visibility curves.

3. STELLAR PARAMETERS

3.1 Phase

The phases of the Mira variables observed were established by means of two sources. Periods were initially obtained from *The General Catalog of Variable Stars, 4th Edition* (GCVS, Kholopov *et al.* 1988). However, since the zero phase date in the GCVS at the epoch of the observations was no less than 11 cycles old for our sample stars, visual brightness data available from the Association Francaise des Observateurs d'Etoiles Variables (AFOEV) was utilized in estimating a recent zero phase date (Schweitzer 1995); for one star (R Peg), data from the American Association of Variable Star Observers (AAVSO) was utilized for this purpose (Mattei 1995).

As an additional cross check, Fourier analysis (as discussed in Scargle 1982 and Horne & Baliunas 1986) of the AFOEV data also provided period information, but using light-curve data which was more recent than that found in the GCVS. The periods from the GCVS and the AFOEV analysis agreed at the 1% level, corresponding to an average difference in period of $1^d.4$. With the agreement in periods, the zero phase estimate was the larger uncertainty in phase determination, although this uncertainty was still small, averaging 6^d with a median of $3^d.5$. Periods, determined from Fourier analysis of the AFOEV data, and phases, from AFOEV and AAVSO data, for each of the Mira variables are presented in Table 1.

3.2 Spectral Type & Bolometric Flux

Bolometric fluxes (F_{BOL}) of the Mira variable stars were estimated from a relationship between F_{BOL}, 2.2 μm flux (F_K) and spectral type, as established by Dyck *et al.* (1974). In order to obtain bolometric fluxes, K magnitudes were first estimated from the incoherent flux levels present in the IOTA data. We obtained our standard star photometric calibrations using the K-band measurements found in the Two Micron Sky Survey (Neugebauer & Leighton 1969) for our nonvariable point-response calibration sources. No airmass corrections were applied since the calibrators were observed at nearly identical airmasses as the Mira variables. In all cases the bolometric fluxes were obtained from the absolute K fluxes through the observed relation between $\log(F_K/F_{BOL})$ and spectral type (Dyck *et al.* 1974), a relationship that requires the phase dependent spectral type for the star. We note that the $\log(F_K/F_{BOL})$-spectral type relationship also has a firm theoretical basis and may be seen in the "infrared flux method" calculations carried out by Blackwell & Lynas-Gray (1994). No reddening corrections were applied to obtain the bolometric fluxes. These were deemed unnecessary since the typical magnitude of the corrections, $\Delta\bar{m}_K = 0.10$ mag (calculated from the empirical reddening determination of Mathis 1990), is less than the rms K-band error, $\bar{\epsilon}_K = 0.15$ mag. The spectral types for the Miras were obtained from the mean observational data of Lockwood & Wing (1971) (hereafter referred to as L&W) and

TABLE 2. Bolometric fluxes and spectral types.

Star	Date	$K\pm\epsilon_K$ [mag]	$F_{BOL}\pm\epsilon_F$ [10^{-8} erg/cm^{2}s]	Spectral Type
R AQL	95 Jun 10	-0.84±0.04	383.0±55.5	M6.5
	95 Oct 06	-0.77±0.03	316.4±45.1	M8.2
R AQR	95 Jul 11	-1.01±0.10	399.2±68.5	M8?
	95 Oct 07	-0.74±0.30	311.3±103.0	M8?
R AUR	95 Oct 03	-0.79±0.02	365.8±51.5	M6.5
X AUR	95 Oct 04	3.83±0.14	5.3±1.1	M6
R CAS	95 Oct 04	-1.29±0.13	447.4±85.2	M9.8
T CAS	95 Oct 04	-0.98±0.06	411.4±62.4	M7
Z CET	95 Oct 06	2.97±0.05	12.5±1.8	M5
S HER	95 Jul 07	1.47±0.11	43.1±7.6	M7
U HER	95 Jun 10	-0.43±0.02	240.8±33.9	M7.5
RY LYR	95 Oct 08	2.79±0.09	12.4±2.1	M7.5
X OPH	95 Jul 07	-1.03±0.10	402.0±68.9	M8.2
	95 Oct 07	-1.05±0.10	414.2±71.0	M8
S ORI	95 Oct 06	0.11±0.01	130.5±18.2	M9
U ORI	95 Oct 08	-0.52±0.02	233.2±32.8	M8.8
R PEG	95 Jul 07	0.50±0.06	98.2±14.9	M8.2
	95 Oct 06	-0.18±0.08	208.6±33.5	M6.5
S PEG	95 Jul 08	1.36±0.51	50.5±26.7	M6.5
	95 Oct 06	1.45±0.04	40.9±5.9	M8.2
R PER	95 Oct 05	4.02±0.19	4.8±1.1	M5
U PER	95 Oct 04	0.97±0.05	64.4±9.5	M8
R SER	95 Jul 07	-0.15±0.07	186.1±29.0	M7.5

References for spectral types in Table 2 are from Lockwood & Wing (1971) and Lockwood (1972).

Lockwood (1972); the cycle-to-cycle repeatability of the phase-dependent spectral types was examined and found to be roughly ±0.25 of a subclass. Spectral types, K magnitudes and bolometric fluxes are given in Table 2. The errors in the K magnitudes are the standard deviations of the individual measurements on a given night. From the observed scatter in the F_K/F_{BOL} relationship we estimate an rms error of ±13% in F_{BOL} from the use of the K magnitude; we estimate a further uncertainty of ±5% in the absolute calibration (Blackwell & Lynas-Gray 1994). The estimated error for F_{BOL} in Table 2 is the quadrature sum of these contributions.

It is also worthwhile to point out that over the range of spectral types in question (M5–M9.8), the $\log(F_K/F_{BOL})$ vs spectral type relationship is nearly flat, making the determination of F_{BOL} robust despite possible inaccuracies in spectral type. An error of two full subclasses results in only a 14% difference in the determined F_{BOL}; we shall see (in Sec. *3.4*) that this results in only a 4% difference in the determined effective temperature. A good example of this is R Aqr, which, at phases of 0.34 and 0.57, did not have a spectral type listed in Lockwood (1972); the range of phases covered for that star in that paper only runs from 0.00 to 0.16. Stars showing similar phase-spectral type behavior in the Lockwood paper at the phase range of 0.00–0.16 (R Aql, T Cas, RU Cyg, X Oph) exhibit a spectral type of roughly M8±1 at a phase of 0.58. Hence, even though a spectral type was not directly available for R Aqr at the phase at which it was observed, a reasonable estimate for its F_{BOL} was still possible.

3.3 True Angular Diameter

In order to estimate effective temperatures, the uniform disk diameters in Table 1 needed to be converted to stellar diameters corresponding to the non-uniform extended atmospheres of the Mira variables. For our purposes here, we used the model Mira atmospheres discussed in Scholz & Takeda (1987) (hereafter referred to as S&T). We note that the S&T models do not account for the time for both shock compressed material and material expanding between shocks to return to radiative equilibrium. These regions, with $T>T_{RadEq}$ and $T<T_{RadEq}$, respectively, can alter the brightness distribution profile and consequently alter the "true" angular sizes derived from the uniform disk diameters. Dynamical atmosphere calculations have the potential to resolve these concerns (e.g., Bowen 1988; Bowen & Willson 1991); however, center-to-limb brightness profiles are not yet available for such calculations. The missing physics in the models has the potential to make for poor agreement between angular sizes derived at different wavelength bands; as we shall see in Sec. *4.5*, this is indeed the case. Noting these concerns, for our purposes here we shall use the S&T models as a sufficient expectation of the intensity distribution across the disk of a Mira variable.

Using the disk intensity distributions given in S&T for their X3500 and X3000 models, visibility curves were computed for these model stars and compared to visibilities for uniform disks. The X3500 and X3000 models of S&T are one solar mass, solar element abundance Mira variable stars with maximum temperatures of 3500 and 3000 K, respectively. Other intermediate-temperature models were referred to in S&T (X3350 & X3200) but, since intensity distributions for these models are not explicitly given, they were not utilized in our analysis. In their discussion of model Mira atmospheres, S&T adopt a radius corresponding to the altitude at which the Rosseland mean opacity equals unity, a convention that shall also be used in this paper.

Our procedure, then, is to convert our uniform disk angular diameters to the corresponding Rosseland mean angular diameters. First, a 2.2 μm uniform- to limb darkened-disk scaling factor, R_{LD}/R_{UD}, was calculated by comparing visibility curves of uniform disk and S&T's limb darkened-disk intensity distributions; R_{LD}/R_{UD} typically resulted in an increase (on average 23%) in calculated size. Second, a limb darkened- to Rosseland disk scaling factor, R_R/R_{LD}, was given in S&T; R_R/R_{LD} typically resulted in a decrease (on average 17%) in calculated size. For 2.2 μm uniform disk diameters, the net R_R/R_{UD} scaling factor is close to unity; this result is consistent with theoretical expectations (Willson 1986). The R_R/R_{UD} scaling factor has been computed for each of the four Mira models used from S&T (X3000 & X3500, minimum & maximum for each).

Stars between a phase of 0.25 and 0.75 were considered to be at minimum; stars between 0.00–0.25, and 0.75–0.99 were considered to be at maximum. Since, as we shall see in Sec. *3.4*, there was not a clear separation between the derived temperatures, the X3000 and X3500 scaling factors were averaged together. For the maximum light models, the X3500 and X3000 R_R/R_{UD} values were 0.97 and 0.99, respectively, (a negligible difference) which were averaged to a maximum light scaling factor of 0.98. For the minimum light models, the R_R/R_{UD} values were 1.05 and 1.17, resulting in a scaling value of 1.11; we note that a full difference of 0.06 (the

TABLE 3. Mira variable effective temperatures.

Star	Date	Model	Scaling	$\theta_R \pm \epsilon_\theta$ [mas]	$T_{EFF} \pm \epsilon_T$ [K]
R AQL	95 Jun 10	MAX	0.98	10.54±0.60	3189±147
	95 Oct 06	MIN	1.11	15.12±0.80	2539±113
R AQR	95 Jul 11	MIN	1.11	16.59±1.03	2568±136
	95 Oct 07	MIN	1.11	15.61±0.80	2489±215
R AUR	95 Oct 03	MAX	0.98	10.84±0.57	3109±137
R CAS	95 Oct 04	MAX	0.98	13.28±0.93	2954±174
T CAS	95 Oct 04	MIN	1.11	14.22±0.73	2795±128
S HER	95 Jul 07	MAX	0.98	4.76±1.15	2749±354
U HER	95 Jun 10	MAX	0.98	10.43±0.78	2855±146
X OPH	95 Jul 07	MIN	1.11	14.40±0.66	2762±134
	95 Oct 07	MAX	0.98	12.06±0.74	3041±160
S ORI	95 Oct 06	MIN	1.11	11.70±0.75	2313±110
U ORI	95 Oct 08	MAX	0.98	10.86±0.56	2776±121
R PEG	95 Jul 07	MAX	0.98	9.98±0.39	2333±100
	95 Oct 06	MAX	0.98	9.53±0.66	2881±153
S PEG	95 Jul 08	MIN	1.11	8.77±0.80	2107±295
	95 Oct 06	MIN	1.11	7.02±1.05	2235±186
U PER	95 Oct 04	MIN	1.11	6.49±0.87	2604±199
R SER	95 Jul 07	MIN	1.11	9.50±0.64	2804±144

difference between 1.11 and the R_R/R_{UD} values for the two minimum light models) in scaling factor results in only a 3% change in the resultant value of T_{EFF}. The corrected angular diameters are listed in Table 3, along with the assumed multiplicative factor to convert uniform disk diameters to Rosseland mean diameters and the S&T models from which they were derived.

The largest scaling factor, $R_R/R_{UD}(MIN)=1.11$, results in only a 5% change in the resultant value of T_{EFF}. Thus, introduction of the uniform disk/Rosseland mean disk scaling factors constitutes merely a perturbation upon the final effective temperature; however, for completeness, they have been included in this study. The analyses found in the next section have been performed with the size scaling noted in this subsection. However, as a cross check, each analysis was repeated without the scaling prescribed by the S&T models, and the gross trends found in the results were unchanged (see Sec. *4.3* for an illustration of this point).

We also note that some consideration was given to the possibility of departures from spherical symmetry in these variable stars. As has been observed in visible light observations of Mira variables (Karovska *et al.* 1991; Haniff *et al.* 1992; Wilson *et al.* 1992), these stars can be considerably elongated, possessing up to a 20% difference between semimajor and semiminor axes. However, this effect appears to diminish at longer wavelengths: In Karovska *et al.*, a 18% difference at 533 nm is accompanied by only a 7% difference at 850 nm. These observations, which were made with a 4 m telescope, will have marginal resolution at the longest wavelength so that the observed decrease in the asymmetry may be the result of loss of resolution. Since the symmetric or asymmetric nature of these stars has at this time not been specifically quantified at 2.2 μm, we have been unable to specifically account for it. The reader should be aware of the potential for this effect to introduce spread in our sample of angular sizes, though it is our expectation that its magnitude will be less than the errors in the data set. We will return to possible effects of asymmetries in Sec. *4.5*.

TABLE 4. Mira variable linear radii.

Star	Date	$\theta_R \pm \epsilon_\theta$ [mas]	D [pc][1]	D [pc][2]	D [pc][3]	$D \pm \epsilon_D$ [pc]	$R \pm \epsilon_R$ [$R_\odot$]
R Aql	95 Jun 10	10.54±0.60		200	190	198±17	224±24
	95 Oct 06	15.12±0.80		200	190	198±17	321±33
R Aqr	95 Jul 11	16.59±1.03	200	230		222±20	396±43
	95 Oct 07	15.61±0.80	200	230		222±20	372±38
R Aur	95 Oct 03	10.84±0.57		260		260±26	303±34
R Cas	95 Oct 04	13.28±0.93		180	230	187±17	267±30
T Cas	95 Oct 04	14.22±0.73		240	350	253±23	386±40
S Her	95 Jul 07	4.76±1.15	590			590±112	302±93
U Her	95 Jun 10	10.43±0.78		350	360	352±31	395±46
X Oph	95 Jul 07	14.40±0.66			270	270±51	418±82
	95 Oct 07	12.06±0.74			270	270±51	350±70
S Ori	95 Oct 06	11.70±0.75		410	480	422±37	530±58
U Ori	95 Oct 08	10.86±0.56		260	240	255±23	298±31
R Peg	95 Jul 07	9.98±0.39	400	410		408±36	437±42
	95 Oct 06	9.53±0.66	400	410		408±36	418±47
S Peg	95 Jul 08	8.77±0.80	640	610		616±55	580±74
	95 Oct 06	7.02±1.05	640	610		616±55	465±81
U Per	95 Oct 04	6.49±0.87		440		440±44	307±51
R Ser	95 Jul 07	9.50±0.64	330	390		373±33	381±42

[1] Jura & Kleinmann (1992); [2] Wyatt & Cahn (1993); [3] Young (1995)

3.4 Effective Temperature

The stellar effective temperature T_{EFF} is defined in terms of the star's luminosity and radius by $L=4\pi\sigma R^2 T_{EFF}^4$. Rewriting this equation in terms of angular diameter and bolometric flux, a value of T_{EFF} was calculated from the flux and Rosseland diameter using

$$T_{EFF}=2341\times\left(\frac{F_{BOL}}{\theta_R^2}\right)^{1/4}; \quad (2)$$

the units of F_{BOL} are 10^{-8} erg/cm^2 s, and θ_R is in mas. The error in T_{EFF} is calculated from the usual propagation of errors applied to Eq. (2). The measured T_{EFF}'s are given in column 6 of Table 3, and are found to fall in the range between 2100 and 3200 K.

3.5 Linear Radius

As with many types of variable stars, Mira variables exhibit a period–luminosity relationship, as first suggested by Gerasimovic (1928). Later work confirmed this relationship (e.g., Clayton & Feast 1969), although in the visible the relationship shows a lot of scatter. To overcome this handicap, methods for determining Mira variable luminosity have been expanded to include both the visible and the infrared (Celis 1980, 1981, 1984; Cahn & Wyatt 1978; Wyatt & Cahn 1983; Robertson & Feast 1981; Feast *et al.* 1989; Jura & Kleinmann 1992, hereafter referred to as J&K). Distances to the Miras in our sample could be estimated by a number of statistical approaches: The period–mass–luminosity relationship developed by Cahn & Wyatt (1978); The infrared period–luminosity relationship developed by Feast *et al.* (1989) as modified by J&K and; the color–absolute magnitude relation of Celis (1980) as applied by Young (1995). J&K give no estimates of the errors in the distances. Using the uncertainties in the constants for the infrared period–luminosity relationship given by Feast *et al.* (1989), we established an average uncertainty of 19% in the J&K distances. For the Wyatt & Cahn (1983) distances, we adopt an uncertainty of 10% in these distances, following the authors' suggestion. For distances from the method of Celis (1980), Young (1995) adopted an uncertainty of 19%; we have adopted this error estimate as well. In Table 4 we have summarized the distances from the three methods and given our

TABLE 5. Previous angular size observations of Mira variable stars.

Star	Date	P (d)	ϕ	Spectral Type	Ref	K	Ref	F_{BOL} [10^{-8} erg/cm^{2}s]	θ_{UD} [mas]	Ref	λ [μm]	$\Delta\lambda$ [μm]	Scaling	θ_R [mas]	T_{EFF} [K]	D [pc]	R [$R_\odot$]
o CET	08/21/90	331.8	0.85	M8.5	1	-2.20	1	1387.44	37.04	4	2.20	0.40	0.98	36.30	2371	89	346
o CET	09/19/90	331.8	0.94	M6.5	1	-2.60	1	2668.17	35.93	4	2.20	0.40	0.98	35.22	2835	89	336
R LEO	05/02/90	313.7	0.21	M7	1	-2.65	3	1592.99	33.00	5	2.16	0.04	1.11	36.63	2443	101	398
S PSC	12/02/76	411.1	0.92	M6.5	2	2.44	3	12.93	3.84	6	2.23	0.14	0.98	3.76	2288	918	371
U ARI	09/03/77	372.0	0.49	M8	2	1.48	3	38.57	6.11	6	1.62	0.42	1.00	6.11	2360	620	407
VV SGR	08/24/77	401.5				1.97	3	30.51	5.21	6	1.62	0.42	1.00	5.21	2410	700	392
VV SGR	05/24/78	401.5				1.97	3	30.51	4.99	6	2.17	0.03	1.00	4.89	2488	700	375

1. Lockwood & Wing 1971; 2. Lockwood 1972; 3. Gezari *et al.* 1993; 4. Ridgway *et al.* 1992; 5. Di Giacomo *et al.* 1991; 6. Ridgway *et al.* 1979

adopted distance and estimated error. The final estimated distance and its error is an average of the independent estimates tabulated, weighted by the errors just discussed.

For the Feast *et al.* (1989) distances taken from J&K, we note two concerns: First, following the suggestion of Wood (1990) concerning LMC versus Milky Way metallicities, J&K argue that local stars are intrinsically fainter at K by 0.25 mag, and modify Feast *et al.*'s M_K-P relationship accordingly; and second, Feast *et al.*'s single line fit for the M_K-P data ignores an "elbow" in the data at approximately $\log P=2.6$, a corner which is also evident in LMC Mira data of Hughes & Wood (1990). Explicit examination of the Feast *et al.* data indicates that true K magnitudes for the longer period variables, including those at the corner, are potentially brighter than those indicated by the simple single line fit. For Mira variables with $\log P=2.57$, which is the average value for the stars in our data set, the actual K magnitudes are potentially brighter by 0.25 mag. Countering the first concern is the argument by Willson *et al.* (1996) that the assumption that local Mira variables are fainter is incorrect. However, the net effect of these two concerns is to cancel each other out, and they are listed herein merely for the sake of completeness. Considering the possibility of these two concerns not completely canceling, the worst case would be a change in K magnitude of the full 0.25 mag, resulting in a difference of 12% in distance, well within the error bars already assigned to the Feast *et al.* distance estimates.

We note that we will ultimately be addressing the question of the pulsation mode (see Sec. 4) for the Mira variables in our sample. Two of the methods for computing the distance (the period–mass–luminosity and the infrared period–luminosity relationship) are dependent upon initial assumptions about the pulsation mode; however, the mean color method developed by Celis (1980) is not. Where there is overlap among the methods, it may be seen from Table 4 that the agreement of the three methods is good. The rather unrelated methods of Celis (1980) and Wyatt & Cahn (1983) shows an average random difference of 20%, comparable to the errors given, with a maximum difference of 46% in the T Cas estimates. Hence, for the purpose of further discussion, we assume that the effect of an assumption about the pulsation mode produces only minor changes in the distance scale.

Once distances to these stars were established, linear radii were then calculated by means of simple geometry. The sizes estimated for these stars are consistent with grossly extended stars in their postgiant evolutionary stage and are in the expected 200–600 $R_\odot$ range (see Hill & Willson 1979; Tuchman *et al.* 1979; Wood 1974). Not listed in Tables 3–5 are two stars which were unresolved, X Aur and Z Cet. Unsurprisingly, the distances for these stars are much greater than for the resolved sources, both being at approximately 950 pc. The mean Mira size, 376 $R_\odot$ would be only 3.7 mas at a distance of 950 pc, well below the smallest observed angular size of 4.85 mas. Even the maximum observed size, 580 $R_\odot$ would still be only partially resolved (5.7 mas) with the projected baselines at which these stars were observed.

3.6 Previously-published Data

As mentioned in the introduction (Sec. 1), six infrared angular size measurements for five stars have been published. We have applied the same reduction procedure discussed in Sec. 3 to the previously published data and have listed the results in Table 5. Errors are not listed in Table 5 but are of the same order as the our own data. Stellar parameters derived from these observations are in good agreement with our own results. For specific stars, there are the following pertinent points:

o Cet (Mira). Observations of this star with the IR Michelson Array (IRMA) were published as a single epoch measurement (Ridgway *et al.* 1992), but for the purposes of this paper, we have separated the data into two epochs: 8/21/90 (ϕ=0.85) and 9/19/90 (ϕ=0.94). We note that the phases calculated for these two epochs were incorrectly listed in Ridgway *et al.* (1992). Spectral type and K band flux for Mira was estimated from phase-dependent values given in L&W. Size scaling of the star's uniform disk angular diameter θ_{UD} to Rosseland diameter θ_R was calculated as discussed in Sec. 3.3; this scaling is different than the scaling applied in Ridgway *et al.* (1992), but is consistent with expected scaling (Ridgway 1996; Haniff 1996). Distances for Mira can be found from trigonometric parallax (van Altena *et al.* 1991) and also from the other indirect estimates (Wyatt & Cahn 1983; Jura & Kleinmann 1992); a weighted average of these measurements was utilized as a reasonable estimate of the true distance of Mira.

R Leo. This star was observed by Di Giacomo *et al.* (1991) via lunar occultation. Spectral type was determined from phase-dependent values given in L&W and the K-band magnitude was estimated from Gezari *et al.* (1993). A distance estimate to R Leo was computed by taking a weighted average of values found in Wyatt & Cahn (1983); Celis (1984), van Altena *et al.* (1991), and Jura & Kleinmann (1992). We note that $T_{\rm EFF}$ and R were determined from the published $\theta_{\rm UD}$ by the methods presented in Sec. 3; compared to the values determined independently by Di Giacomo *et al.* (1991), they agree to within 1% and 5%, respectively.

S Psc, U Ari, VV Sgr. The angular diameters for these stars were determined by Ridgway *et al.* (1979) by lunar occultation, with VV Sgr being observed twice (1977 August 24 & 1978 May 24). Determination of the phase of VV Sgr was not possible; light-curve data was not available, and the zero epoch data in the GCVS was 50+ cycles old. Spectral types for S Psc and U Ari were determined from phase-dependent values given in L&W and Lockwood (1972); the K-band magnitude for each of the three stars was estimated from values in Gezari *et al.* (1993). The U Ari observations were in the J band; a 1.6 μm $\theta_{\rm UD}$ to θ_R scaling factor was calculated using the pertinent data from S&T, using the method discussed in Sec. 3.3. For both of the observations of VV Sgr, a scaling factor of 1 was employed since determination of phase was not possible. A distance estimate to S Psc was found in Onaka *et al.* (1989), who used their method of modeling dust shell spectra; distance estimates of U Ari are in Wyatt & Cahn (1983); Jura & Kleinmann (1992). A distance estimate to VV Sgr can be found in Nguyen-Q-Rieu *et al.* (1979), who utilized the period-mean maximum visual absolute magnitude relationship found in Clayton & Feast (1969) and Foy *et al.* (1975); however, the indicated value of 1375 pc results in a linear diameter more than a factor of 2 larger than diameters for other Mira variables of the same type. Alternatively, we may estimate its distance from the distances derived for the other stars in the sample, under the crude assumption that all Miras have equal K luminosities. This method results in a distance of 700 pc which produces a more consistent value for the radius; we adopt this value for the remainder of the discussion.

4. DISCUSSION

4.1 Relationships among the Derived Quantities

Now that we have established values for the basic properties of phase, spectral type, bolometric flux, effective temperature, and radius for the Mira variables we observed, we will investigate possible relationships between these basic stellar parameters. We must stress that treating the Mira variables as identical stars is a crude assumption; however, we are attempting to investigate the gross behavior of these similar stars. We also note that, aside from radius, these parameters are the direct result of observational data and do not make any assumptions about the pulsation mode of the stars. As we mentioned above, two of the approaches for deriving distances, and hence linear radii, presume to varying extents fundamental mode pulsation; however, we reiterate that the third approach of Celis avoids such assumptions and produces numbers in rough agreement with the first two methods.

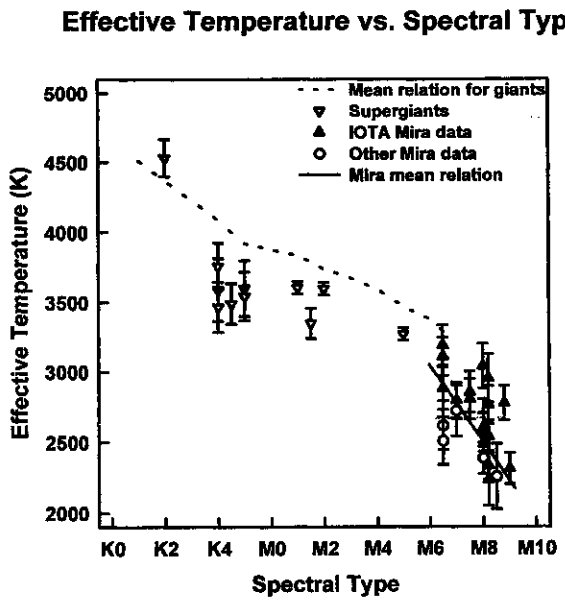

FIG. 1. A plot of effective temperatures vs spectral type for the Mira variables observed, and corresponding giant/supergiant data from Dyck *et al.* (1996).

4.2 Effective Temperature Versus Spectral Type

In a previous paper (Dyck *et al.* 1996), we used angular size measurements from the IOTA interferometer to investigate the dependence of $T_{\rm EFF}$ upon spectral type for a large sample (66) of giant and a smaller sample (11) of supergiant stars. Our results refined the mean $T_{\rm EFF}$-spectral type relationship for giant stars from the spectral types K1 through M7. The data set on luminosity class I and I-II stars in our sample indicated that they are roughly 400 K cooler than their giant counterparts at a spectral type of K4.5; the data suggested that the effective temperature difference between supergiants and giants approaches zero as the spectral type approaches to M6. In contrast, the Mira variables observed for this paper are considerably cooler than their giant counterparts at spectral types later than M6.

For stars with effective temperature errors less than 250 K, we have plotted the spectral type and effective temperature data in Fig. 1, where we have included, for comparison, the earlier results obtained for K and M giants and supergiants. The mean value of the effective temperature as a function of spectral subclass is listed in Table 6 for those Mira variables shown in Fig. 1. The errors listed were obtained from the standard deviation of the temperatures at each spectral subtype. For the undersampled spectral subclasses M7.0 and M7.5, the error listed in Table 6 has been estimated from the average error for better-sampled spectral subclasses (M6.5, M8.0, M8.2), and scaled by $\sqrt{5/2}$ to account for differences in sample size. The data from sub-

TABLE 6. Mean effective temperatures.

Spectral Type	Mean $T_{EFF}\pm\sigma_T$ (K)	Fitted $T_{EFF}\pm\sigma_T$ (K)[2]
M6.5	2900±270	2910
M7.0	2770±410[1]	2770
M7.5	2830±410[1]	2640
M8.0	2580±225	2500
M8.5	2520±280	2380

1. Error estimate (see §4.2).
2. T_{EFF} = (M subclass) * (-273 ± 40) + (4690 ± 530) *K*

classes M8.2–M9.0 has been collected together for a single estimate of T_{EFF} at subclass M8.5.

Although the errors listed in T_{EFF} listed in Table 6 are sizable, a great deal of the spread could be due to inaccuracies in determination of spectral subclass for the Miras observed. Since the spectral classifications were inferred rather than directly determined contemporaneously, the possibility of slight misclassification exists. Examining the multiple epoch data of L&W and Lockwood (1972), there appears to be approximately a half to full subclass of spread in the classification for stars as they pass through a given phase point. As a consequence, the errors on spectral type were assumed to be ±0.33 for the stars in our sample, except for R Aqr, which as noted in Sec. *3.2* was assumed to be ±1.0. A rudimentary line fit to our T_{EFF}-spectral type data (accounting for errors in both spectral type and T_{EFF}) results in a fit of T_{EFF}=(M subclass)*(−273±40)+(4690±530) *K*, with a reduced χ^2=2.47. As evidenced by the χ^2, the fit is indeed rudimentary, but the gross result is that a change on one spectral subclass would affect a change of roughly $\Delta T_{EFF}\approx$300 K. Contemporaneous spectral typing thus has the potential to greatly reduce the scatter in T_{EFF}-spectral type relationship.

Note that the Mira variables are substantially cooler than the giant stars of the same spectral type. At spectral type M7 the Mira scale is offset to lower temperatures by nearly 400 K; at M8 the Mira scale is about 350 K cooler than the temperature of RX Boo, an M8 giant. These results are a general extension of the earlier finding that the more luminous stars are systematically cooler than the less luminous ones (Dyck *et al.* 1996).

4.3 Effective Temperature Versus Phase

We expect from the photometric and spectroscopic studies that the effective temperature of a Mira variable will change during its cycle of variability. As described in Secs. *3.1* and *3.4*, phase and temperature as a function of phase have been determined for each of the Mira variables observed at IOTA. We have plotted the data for all the stars in Fig. 2, where clearly there is a lot of scatter resulting from the poor assumption that the stars are all identical. Nevertheless, we may see a clear trend when the data are averaged into phase bins; this is shown in the figure as a solid line.

As a comparison we have taken the L&W and Lockwood (1972) observations of the spectral types of several of the stars we observed (R Aql, o Cet, S Her, U Her, X Oph, R Peg) made over several cycles, converted them to effective

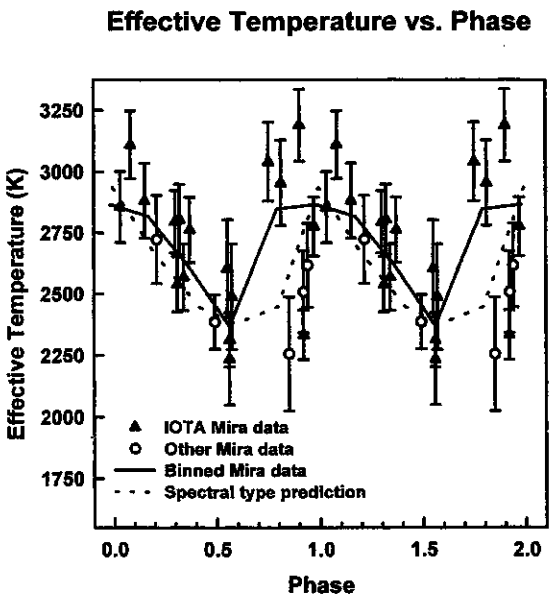

FIG. 2. Effective temperature as a function of phase, including data obtained on this program and data previously published for five other Mira variables. Bin size for both the observed Mira variables and the predicted Mira variable behavior is 0.2 of a period. The predicted temperatures have been estimated from the T_{EFF}-spectral type relation illustrated in Fig. 1 and the phase-dependent spectral type data of Lockwood & Wing (1971) and Lockwood (1972).

temperatures using the linear relation described in Sec. *4.2*, averaged the results and plotted the averages in Fig. 2 as a dashed line. One may see that the expected variation of the effective temperature, based upon the L&W and Lockwood (1972) data, is such that it peaks slightly after maximum visible light (at phase ≈0.1) and has its minimum near phase 0.6–0.7; the amplitude of the variation is about 400 K, ranging from 2500 to 2900 K. Averages of our heterogeneous data are consistent with these patterns; we note that the greatest deviation between the two sets of T_{EFF} data is at a phase of 0.7, where our data is the most sparse.

As was mentioned in Sec. *3.3*, our analysis was repeated for temperatures obtained without the use of angular size scaling. A plot of these temperatures, not repeated here, showed the same level of scatter and trends as the temperatures determined from the Rosseland-scaled diameters so that the effective temperatures are insensitive to this level of size scaling. This is consistent with expectation that near infrared uniform disk diameters should be reasonable as direct indicators of the true photospheric diameters of Mira variables (Willson 1986).

4.4 Radius Versus Effective Temperature

It is also of interest to plot radius versus effective temperature, which we have done in Fig. 3. Although there is considerable spread with the uncertainty shared between T_{EFF} error and the error in distance measurements, to first order the relation appears linear. For the purpose of further

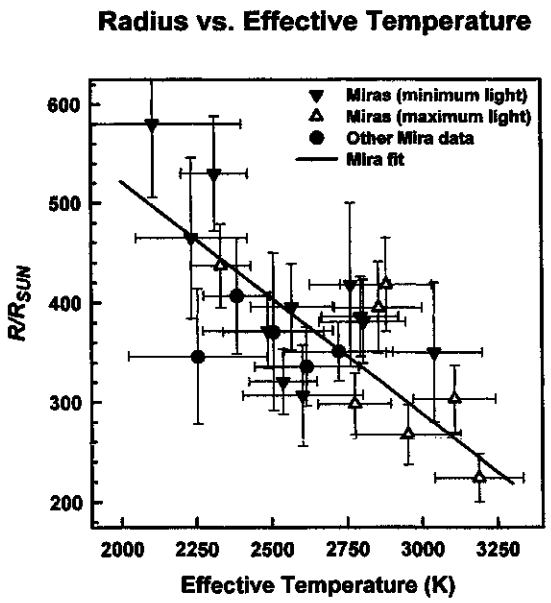

FIG. 3. Mira variable radius vs effective temperature. To first order these parameters appear to be linearly interrelated for these stars. Initial multiepoch data supports the hypothesis that these stars are varying along this line over the course of their periods.

discussion, an error-weighted two-dimensional linear least-squares fit was performed upon the sample, with the following result:

$$R = 405 \pm 16 R_{\odot} - 0.233 \pm 0.004 \frac{R_{\odot}}{K} \times (T_{\mathrm{EFF}} - 2500 \quad \mathrm{K}), \tag{3}$$

with a reduced chi-square of 0.94.

Suppose that Miras variables, to first order, over the course their cycles oscillate along the line segment fit to the data, with their amplitudes limited by the observed locus of data points. We can use our line fit to specify surface area as a temperature dependent quantity; the product of that area and the Planck function gives the total power at any wavelength for a given temperature. The range of temperatures can be estimated from the observed phase-dependent variation; in Sec. *4.3* the variation was indicated to be approximately 400 K, between 2500 and 2900 K. The fit of Eq. (3) indicates a size range of 405 $R_{\odot}$ to 310 $R_{\odot}$ from minimum temperature to maximum temperature, a variation of roughly 25%, which is consistent with our observed radius variations. Under this hypothesis, three features are predicted to be seen in Mira variable observational data as the temperature varies. First, the visible light flux reaches extremes at either edge of the temperature range, maximizing at a temperature of about 2900 K and minimizing at about 2500 K. The difference in flux over the course of the cycle corresponds to a factor of 2.9, or approximately 1.2 mag. Second, the K flux peaks at about 2500 K, and reaches minimum value at about 2900 K. In this wavelength band, the difference in flux corresponds to a factor of 1.1, or about 0.14 mag. Third, since the two wavelength bands peak at separate temperatures, the V- and K-band maxima exhibit a phase shift relative to one another during a Mira's cycle. A cursory examination of our result indicates that the value of the phase lag is approximately 0.5.

Each one of these three predicted characteristics of Mira variables is in gross agreement with the actual observed behavior of Mira variables. The observed variation of a Mira variable in the V band ranges from $\Delta V \simeq 2.5$ mag up to $\Delta V \simeq 6$ mag for the more extreme Mira variables (e.g., R Cas). Examining the K-band light curves presented in L&W, we find a diminished K-band variability relative to the V-band variability. The K-band variation seen in the limited L&W infrared data is in the $\Delta K \simeq 1$ mag range. Also, the delay of maximum with increasing wavelength is a well-known characteristic of Mira variables (Pettit & Nicholson 1933; L&W; Barnes 1973); L&W observed the K-band lag to be approximately 0.1–0.2. For each of the three light-curve characteristics expected from our simple hypothesis, there is poor specific agreement between the observations and the expectations (e.g., $\Delta K_{\mathrm{observed}} \simeq 1$ mag vs $\Delta K_{\mathrm{predicted}} \simeq 0.14$ mag); however, the gross agreement (e.g., phase lag prediction, diminished K variability) indicates that to first order the simple line fit begins to explain the behavior of the stars. Higher-order perturbations upon the line fit have the potential to refine the agreement between the specific numeric predictions and the observed data; such perturbations will be calculatable when further multiple epoch data becomes available.

As an observational check of this hypothesis, the sample of two-epoch data we have at present (R Aql, R Aqr, X Oph, R Peg, S Peg, and o Cet data from Ridgway *et al.* 1992) can be plotted on a similar illustration as Fig. 3; the changes observed in the effective temperatures and radii for these stars is entirely consistent with this hypothesis and can be seen in Fig. 4. For the stars observed at IOTA, there is an average $\Delta\phi = 0.31$ (range 0.23–0.41), whereas Ridgway *et al.*'s o Cet data has $\Delta\phi = 0.09$.

4.5 Oscillation Mode

The results presented in this paper have the potential to constrain the ongoing debate regarding the pulsation of Mira variables. Specifically, the common lament is for improved values for effective temperatures and radii (see Ostlie & Cox 1986; Perl & Tuchman 1990). As an initial evaluation using our data, we examine the period–mass–radius (PMR) relations developed by Ostlie & Cox (1986, hereafter referred to O&C) by means of a linear pulsation study. For fundamental mode and first-overtone pulsators, respectively:

$$\log P = -1.92 - 0.73 \log M_0 + 1.86 \log R,$$
$$\log P = -1.60 - 0.51 \log M_1 + 1.59 \log R. \tag{4}$$

From these two relations, estimates of the oscillation mode can be calculated for a star of known mass, given observations of period and radius, with the caution that these relations generally apply to a mean radius for the star. We have plotted our radius and period data in Fig. 5 along with the O&C relationships for fundamental and first-overtone pulsations; stellar mass is listed as a parameter for each of the pulsation modes. Shown for comparison are the visible HS&T results, and the infrared data for the other five stars

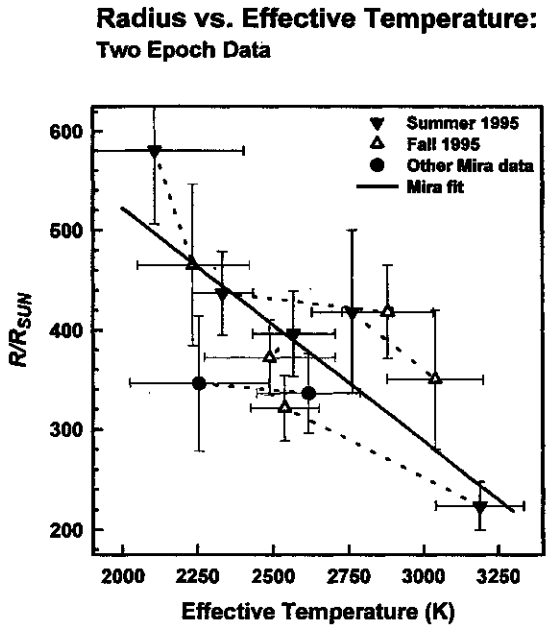

FIG. 4. As Fig. 3, but for the five stars for which multiple epoch data has been obtained. Multiple epoch data on o Cet from Ridgway *et al.* (1992) have also been plotted. For the stars observed at IOTA, approximately one third of a period has elapsed ($\Delta\phi$=0.31, range 0.23–0.41), whereas Ridgway *et al.*'s o Cet data have $\Delta\phi$=0.09.

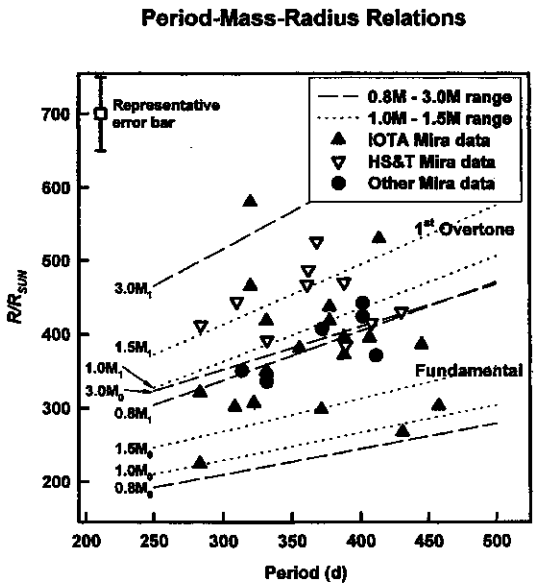

FIG. 5. A plot of the derived radius and period data. Overplotted is the visible-light Mira data of Haniff *et al.* (1995) and the previously-published infrared data for the five other stars discussed in the text. Lines indicate regions for fundamental and first overtone masses for both 0.8–3.0$\mathcal{M}_\odot$ (dash) and 1.0–1.5$\mathcal{M}_\odot$ ranges (dot), as determined by the period–mass–radius relations of Ostlie & Cox (1986). Mass increases with radius for a given mode and period.

taken from the literature (as discussed in Sec. *3.6*). Results from other PMR relations developed by Fox & Wood (1982) and Wood (1990) were also evaluated, producing essentially the same results.

Using the O&C relations to determine the oscillation mode of a Mira variable requires that an acceptable range of masses for the stars be specified. These are generally established by statistical arguments based upon numbers, galactic distribution and expected lifetimes. There is not general agreement for the Mira variables: Willson (1982), Wood (1982), and Willson (1986) favor a mass range 0.8 $\mathcal{M}_\odot<\mathcal{M}<3.0\mathcal{M}_\odot$ while HS&T prefer 1.0 $\mathcal{M}_\odot<\mathcal{M}<1.5\mathcal{M}_\odot$ based upon arguments about mass loss (Knapp & Morris 1985). The choice of mass range has interesting consequences. In Fig. 5 we designate by lines the regions for the two mass limits which support first-overtone and fundamental oscillation modes. In this figure we have plotted our data as well as the visible light data from HS&T. For the wider mass range cited above, we find that our infrared data lie in both the first-overtone and fundamental oscillation mode regions. For the narrow mass ranges, we see that our data lie primarily between the regions indicating fundamental and first-overtone modes. Also, since a certain amount of spread in our radius data could be due to distance errors and potential stellar asymmetries, we can attempt to circumvent these effects by examining our data set as a whole. The unweighted average radius is 376±86 $R_\odot$, and the unweighted average period is 363±51 days (unweighted since the dominant source of radius error is typically a 20% distance error); the indicated mass and mode of this composite data point could be taken to be either fundamental mode, on the high end (~3.0 $\mathcal{M}_\odot$), or first overtone, on the low end of masses (~0.8 $\mathcal{M}_\odot$). For these reasons we favor the larger range of masses.

Note that the HS&T radii lie within our sample but all at the high end of the range of the radii. The mean radius from the HS&T study is 443 $R_\odot$ and from our study is 376 $R_\odot$ (with unweighted standard deviations of 43 $R_\odot$ and 86 $R_\odot$, respectively); that is, the HS&T radii are 18% larger than ours in the mean. In contrast to our finding of either/neither oscillation mode, dependent upon the mass range chosen, HS&T's results strongly indicated first-overtone oscillation, due to the larger indicated diameter from their visible light data. As a verification of our interferometric data, the other infrared size data was examined for significant deviations from our results; the mean of 368 $R_\odot$, with a standard deviation of 39 $R_\odot$, is entirely consistent with our observations. The conclusion of HS&T strongly indicated that a narrow mass range is appropriate for Mira variables; the different conclusions between our study and that of HS&T is troubling and may be examined further.

We note that the data of HS&T incorporates, for each star, multiple epochs of data without any apparent discrimination for the proximity of these stars to maximum or minimum. Hence, the radii determined by HS&T are in certain cases averaged, in the presence of even coverage throughout the cycle. A net result would be the reduction of overall spread in their data set, indicating a 1.0$\mathcal{M}_\odot<\mathcal{M}<1.5\mathcal{M}_\odot$ mass range, narrower than the range indicated by our single epoch data. While an average Mira radius might actually be more appropriate for establishing stellar mass within the context of PMR relations, we note that our data set average is outside

the narrow mass range for either fundamental or first-overtone pulsation, as discussed above.

An important source of errors arises from the lack of geometrically determined distances. This is likely to scale the whole set of radii, rather than to move the HS&T sample selectively with respect to ours. In Sec. *3.3*, we noted that observations of o Cet (Karovska *et al.* 1991) indicated up to a 20% asymmetry in the photospheric extension, a difference coincidentally close to the difference in mean radii between our study and the HS&T study. Could this be the cause of the difference between our observations and the optical wavelength data of HS&T? If this were to be the case, we would need to observe the minor axis preferentially and HS&T the major axis preferentially, an unlikely circumstance.

Independent of the distance estimates, however, we can compare angular diameters of stars common to both data sets. There are three stars common to the two data sets: R Aql, R Cas, and U Ori. The angular diameters of these stars derived by HS&T are systematically larger than ours by a factor of 1.76 ± 0.16. Although small-number statistics could produce a systematic difference for the three stars, one clearly expects some larger and some smaller radii if the result is purely statistical. We may also examine the relative angular diameters for the three stars, normalizing the values to the radii of R Aql presented in our respective data sets; we find

$$\text{R Cas:U Ori:R Aql} = \begin{Bmatrix} 1.42 \pm 0.27 : 1.06 \pm 0.26 : 1.00 \pm 0.30 & \text{HS\&T} \\ 1.26 \pm 0.11 : 1.03 \pm 0.08 : 1.00 \pm 0.08 & \textit{This paper.} \end{Bmatrix}$$

We note that the "E model" θ_R values that HS&T preferred have been used in the comparison; also, our $\phi = 0.90$ R Aql data have been used in the comparison, which is consistent with HS&T's $\phi = 0.06$ R Aql data (both data points are at maximum light); also, the R Cas and U Ori data are at maximum light for both HS&T and the data presented in this paper. This result, which is more or less scaling independent, is indicative of the general observational agreement between our data sets and that more appropriate Rosseland mean scaling factors would produce closer final results. As was noted in Sec. *3.3*, the lack of existing models to account for certain aspects of the stellar pulsation physics has the potential for poor agreement between Rosseland diameters derived from differing wavelengths; the general observational agreement between HS&T's and our data sets is a strong indication that more complete Mira variable models are necessary for achieving complete agreement between the two data sets.

Comparison of the two data sets to the recent dynamic atmospheres models of Bowen (1988, 1996), also indicates that the models utilized are incompletely describing the brightness profiles of these stars. Close agreement of the P-L relationship from the Bowen models with the observed P-L data (Willson *et al.* 1996) strongly suggests that dynamic models are necessary for reconciling not only the two data sets, but observational data in general with theoretical expectations. Comparing the Bowen P-L relation (in the form of a P-R relation) to both our data and HS&T's (Willson 1996), both sets derive radii in excess of that expected from the Bowen models. From the expected size at an average period of $\log \bar{P} = 2.56$, the HS&T E model data are too large by an average 160 $R_\odot$, while our data at $\log \bar{P} = 2.57$ are too large by an average 94 $R_\odot$. The agreement of the Bowen models with the observed P-L data, and the disagreement of our data and HS&T's, suggest that brightness profiles from dynamic pulsation models will be necessary to reduce the interferometric data with greater accuracy. Additional evidence arises from the fact that the S&T models are unable to yield the same Rosseland mean radius for each of the wavelengths used in the HS&T study (Tuthill 1996).

One further concern regarding use of relations such as those derived by O&C is the argument by Ya'ari & Tuchman (1996) that pulsation features of long-period variables cannot be predicted by linear analysis, but only by full, nonlinear hydrodynamic models. PMR relations, or any similar relations accessible to the data in our sample set, unfortunately do not yet exist for nonlinear models.

In spite of the many possibilities for uncertainty, we are encouraged by the lower limit of the PMR data. Note of our lowest mass fundamental mode-indicated oscillators dip below the 0.8 $\mathcal{M}_\odot$ lower edge. We note that an extension of the upper end of the Mira variable mass range to 4.0 $\mathcal{M}_\odot$ would include all but two of our stars in the fundamental mode (S Ori, S Peg being the exceptions), though at this point the regions occupied by two modes begins to overlap seriously.

5. CONCLUSIONS

The IOTA program of observing Mira variable stars has resulted in a much greater number of near-infrared angular size measurements for Miras; previous results were available for only five of these stars. Determinations of $T_{\rm EFF}$ and radius are possible with the caveat that the radii depend upon poorly-known distances; we have established an effective temperature-spectral type relationship for the range M6.5–M8.5. The period-dependent temperature and radius variations of these stars are interrelated, as would be expected. The atmospheric models that are utilized in reducing the visibility data clearly play a significant role in the results obtained; the inability of current models to describe the complex extended atmospheres of these stars precisely at all wavelengths is highlighted by the disagreement between our infrared results and HS&T's visible results. Although our data indicate that Mira variables may oscillate in both fundamental and first-overtone modes, depending upon the star, the disagreement with the HS&T results indicates that it may be premature to draw firm conclusions about the oscillation mode from the angular diameter data. However, our data would appear to agree with estimates that the mass range for Mira variables is 0.8–3.0 $\mathcal{M}_\odot$.

We would like to thank the staff at the Center for Astrophysics for a generous allotment of telescope time so that this project could be carried out, and Ron Canterna for liberal use of computer resources for data reduction. We acknowledge fruitful discussions with Chris Haniff, Peter Tuthill, Lee Ann Willson, and David Ciardi. Our thanks to the

referees—who advised us in considerable detail how to improve this paper. This research has been partially supported by NSF Grant No. AST-9021181 to the University of Wyoming, the Wyoming Space Grant Consortium, and NASA Grant No. NGT-40050. This research has made use of the SIMBAD database and the AFOEV database, both operated by the CDS, Strasbourg, France. In this research, we have used, and acknowledge with thanks, data from the AAVSO International Database, based on observations submitted to the AAVSO by variable star observers worldwide.

REFERENCES

Barnes III, T. G. 1973, ApJS, 25, 369
Barthès, D., & Tuchman, Y. 1994, A&A, 289, 429
Blackwell, D. E., & Lynas-Gray, A. E. 1994, A&A, 282, 899
Bowen, G. H. 1988, ApJ, 329, 299
Bowen, G. H., & Willson, L. A. 1991, ApJ, 375, L53
Bowen, G. H. 1996, in preparation
Cahn, J. H., & Wyatt, S. P. 1978, ApJ, 221, 163
Cannizzo, J. K., Goodings, D. A., & Mattei, J. A. 1990, ApJ, 357, 235
Carleton, N. P., *et al.* 1994, Proc. SPIE, 2200, 152
Celis, S. L. 1980, A&A, 89, 145
Celis, S. L. 1981, A&A, 99, 58
Celis, S. L. 1984, AJ, 89, 1343
Clayton, M. L., & Feast, M. W. 1969, MNRAS, 146, 411
Di Giacomo, A., Lisi, F., Calamai, G., & Richichi, A. 1991, A&A, 249, 397
Dyck, H. M., Benson, J. A., van Belle, G. T., & Ridgway, S. T. 1996, AJ, 111, 1705
Dyck, H. M., *et al.* 1995, AJ, 109, 378
Dyck, H. M., Lockwood, G. W., & Capps, R. W. 1974, ApJ, 189, 89
Feast, M. W., Glass, I. S., Whitelock, P. A., & Catchpole, R. M. 1989, MNRAS, 241, 375
Fox, M. W., & Wood, P. R. 1982, ApJ, 259, 198
Foy, R., Heck, A., & Mennessier, M. O. 1975, A&A, 43, 175
Gerasimovic, B. P. 1928, Proc. Natl. Acad. Sci. USA, 14, 963 (Harvard Reprint 54)
Gezari, D. Y., Schmitz, M., Pitts, P. S., & Mead, J. M. 1993, Catalog of Infrared Observations, NASA Reference Publication 1294
Haniff, C. A., Ghez, A. M., Gorham, P. W., Kulkarni, S. R., Matthews, K., & Neugebauer, G. 1992, AJ, 103, 1662
Haniff, C. A., Scholz, M., & Tuthill, P. G. 1995, MNRAS, 276, 640 (HS&T)
Haniff, C. A. 1996 (private communication)
Hill, S. J., & Willson, L. A. 1979, ApJ, 229, 1029
Hoffliet, D. 1982, Catalog of Bright Stars (Yale University Press, New Haven)
Horne, J. H., & Baliunas, S. L. 1986, ApJ, 302, 757
Hughes, S. M. G., & Wood, P. R. 1990, AJ, 99, 784
Jura, M., & Kleinmann, S. G. 1992, ApJS, 79, 105 (J&K)
Karovska, M., Nisenson, P., Papaliolios, C., & Boyle, R. P. 1991, ApJ, 374L, 51
Kholopov, P. N., *et al.* 1988 General Catalog of Variable Stars, 4th ed. (Nauka, Moscow) (GCVS)
Knapp, G. R., & Morris, M. 1985, ApJ, 292, 640
Lockwood, G. W. 1972, ApJS, 209, 375
Lockwood, G. W., & Wing, R. F. 1971, ApJ, 169, 63
Mathis, J. S. 1990, ARA&A, 28, 37
Mattei, J. A. 1995, Observations from the AAVSO International Database (private communication)
Neugebauer, G., & Leighton, R. B. 1969, Two-Micron Sky Survey, NASA SP-3047
Nguyen-Q-Rieu, M., Laury-Micoulaut, C., Winnberg, A., & Schultz, G. V. 1979, A&A, 75, 351
Onaka, T., De Jong, T., & Willems, F. J. 1989, A&AS, 81, 261
Ostlie, D. A., & Cox, A. N. 1986, ApJ, 311, 864 (O&C)
Pettit, E., & Nicholson, S. B. 1933, ApJ, 78, 320
Perl, M., & Tuchman, Y. 1990, ApJ, 360, 554
Ridgway, S. T., Benson, J. A., Dyck, H. M., Townsley, L. K., & Hermann, R. A. 1992, AJ, 104, 2224
Ridgway, S. T., Wells, D. C., Joyce, R. R., & Allen, R. G. 1979, AJ, 84, 247
Ridgway, S. T. 1996 (private communication)
Robertson, B. S. C., & Feast, M. W. 1981, MNRAS, 196, 111
Rowan-Robinson, M., & Harris, S. 1983, MNRAS, 202, 767
Scargle, J. D. 1982, ApJ, 263, 835
Scholz, M., & Takeda, Y. 1987, A&A, 186, 200 (S&T)
Schweitzer, E. 1995, Observations from the AFOEV Database, private communication
Tuchman, Y. 1991, ApJ, 383, 779
Tuchman, Y., Sack, N., & Barkat, Z. 1979, ApJ, 234, 217
Tuthill, P. G. 1994, Ph.D. dissertation, University of Cambridge
Tuthill, P. G. 1996 (private communication)
van Altena, W. F., Lee J. T., & Hoffleit, E. D. 1991, in The General Catalogue of Trigonometric Stellar Parallaxes (1991): a Preliminary Version (Yale University Observatory, New Haven)
Willson, L. A., & Hill, S. J. 1979, ApJ, 228, 854
Willson, L. A., 1982, in Pulsation in Classical and Cataclysmic Variable Stars, edited by J. P. Cox and C. J. Hansen (JILA, Boulder, CO), p. 269
Willson, L. A. 1986, in Late Stages of Stellar Evolution, edited by S. Kwok and S. R. Pottasch (Reidel, Dordrecht), p. 253
Willson, L. A., Bowen, G. H., & Struck, C. 1996 in From Stars to Galaxies, ASP Conf. Ser. Vol. 98, edited by C. Leitherer, U. Fritze-v. Alvensleben, and J. Huchra (ASP, San Francisco)
Willson, L. A. 1996 (private communication)
Wilson, R. W., Baldwin J. E., Buscher D. F., & Warner P. J. 1992, MNRAS, 257, 369
Wood, P. R. 1982, in Pulsation in Classical and Cataclysmic Variable Stars, edited by J. P. Cox and C. J. Hansen (JILA, Boulder, CO), p. 284
Wood, P. R. 1990, in From Miras to Planetary Nebulae: Which Path for Stellar Evolution?, edited by M. O. Mennessier and A. Omont (Editions Frontières, Gif-sur-Yvette), p. 67
Wood, P. R. 1974, ApJ, 190, 609
Wyatt, J. H., & Cahn, S. P. 1983, ApJ, 275, 225
Ya'ari, A., & Tuchman, Y. 1996, ApJ, 456, 350
Young, K. 1995, ApJ, 445, 872